Theoret. Chim. Acta (Berl.) 65, 109–125 (1984)

THEORETICA CHIMICA ACTA

Theoretical study of hydrogen abstraction reactions $CH_4 + R \rightarrow CH_3 + HR$, geometrical, energetical and kinetical aspects

Michel Sana*, Georges Leroy and José Luis Villaveces*****

Université Catholique de Louvain, Laboratoire de Chimie Quantique, Bâtiment Lavoisier, Place Louis Pasteur, 1 1348 Louvain-la-Neuve, Belgium

Five hydrogen abstraction reactions, $CH_4 + R \rightarrow CH_3 + HR$ have been studied using *ab initio* SCF and CI methods. R was successively chosen as H, CH_3, NH_2, OH and F. Geometries were fully optimized at SCF level and energies were computed at CI level for products, reactants and transition states. Quadratic hypersurfaces were fitted in the neighborhood of the most important points of the potential energy hypersurfaces and vibrational analysis were performed thereupon. Wigner's and Christov's approximations were used to obtain an idea of the importance of tunneling of H atoms through the reaction barrier, and this effect was shown to be non-negligible. Finally, rate constant calculation were carried out at different temperatures.

Key words: Hydrogen abstraction reactions—rate constant—tunneling correction—transition state

Introduction

Hydrogen abstraction reactions involving OH, H and CH_3 have retained the attention of chemists during the last two decades, and many thermochemical and kinetical results concerning them have been published. This includes several comprehensive studies, critically reviewing experimental data, or providing rationalizations of free-radical reaction properties. References [1–8] are examples

* Chercheur Qualifié au Fonds National Belge de la Recherche Scientifique.

** *Offprint requests to*: G. Leroy

*** Present address: Seccion de Fisico-Quimica, Universidad Nacional de Colombia, Ciudad Universitaria, Edificio de Quimica, Bogota D.E. Colombia.

by no means exhaustive of the latter. Their study is an important step towards the understanding of the fundamental problem of stability and reactivity of free-radicals [1], which control many processes in all branches of pure and applied chemistry.

A certain number of theoretical papers devoted to their study have been recently published [9–19] and more or less elaborate quantum chemical calculations are beginning to give theoretical explanations for the general rules based on empirical generalizations or on simple models.

The aim of this work is to study in a theoretical *ab initio* way some hydrogen abstraction reactions.

Five reactions were chosen: the abstractions of hydrogen from methane by the following species: H, CH_3, NH_2, OH and F:

I $\quad CH_4+H\rightarrow CH_3+H_2$

II $\quad CH_4+CH_3\rightarrow CH_3+CH_4$

III $\quad CH_4+NH_2\rightarrow CH_3+NH_3$

IV $\quad CH_4+OH\rightarrow CH_3+H_2O$

V $\quad CH_4+F\rightarrow CH_3+HF.$

We shall refer to them by R, the general case being:

$CH_4+R\rightarrow CH_3+HR.$

Geometries were fully optimized, with special attention focused on the transition states. Energies, force constants, vibration modes and thermal behavior of the activated complex as well as of reagents and products were studied.

1. Potential energy surface

SCF calculations have been carried out in the 6-31G basis set of Pople [20] using the UHF method of Nesbet [21]. The program GAUSSIAN-70 [22] implemented by Schlegel for force calculations [23] was employed.

Around any stationary points (reactants, transition states, products), we develop the Born–Oppenheimer potential energy surface in Taylor series up to the second order:

$$V(S) = V_0 + g_0' S + \tfrac{1}{2} S' H_0 S \qquad (1)$$

where S stands for the column vector of the internal displacement coordinates from the expansion origin; g_0 stands for the gradient vector at $S=0$; H_0 stands for the second order derivative matrix at $S=0$.

The elements of g_0, H_0 and V_0 can be considered as parameters for the polynomial model (1). Experimental planification gives an optimal strategy to estimate them. In case of least square fitting, there exists a point distribution in the internal

space which leads to unbiased estimates of relation (1) warranting a lowest variance of the regression parameters [24–26]. The local surface fitting have been performed in two steps. Firstly we localize the stationary point using large variations on the internal variables around an initial guess:

$$S_e = S \text{ (where } g = 0) = -H_0^{-1} g_0. \tag{2}$$

Secondly, we restrict the variations around S_e to obtain a more accurate estimation of H_0 less aliased by third or fourth order terms not contained in (1). This second turn is important for further vibrational analysis.

In Fig. 1, we report the internal coordinate definition. So, for transition structures, we have between 9(CH_4+H) and 21(CH_4+CH_3) degrees of freedom ($k = 3N - 6$) to be considered simultaneously. In Table 1, we give the geometrical properties associated to the different stationary points. Compared to the experimental results, we see that the bond lengths are nicely reproduced at the SCF level. However, this is not quite true for the valence angles if they are not symmetry

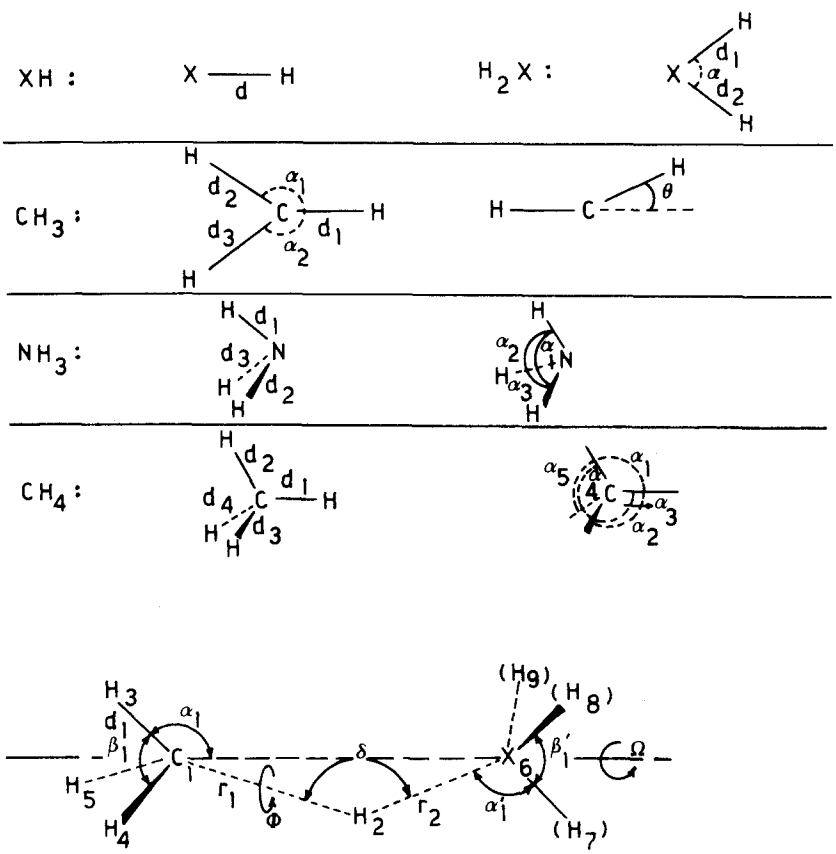

Fig. 1. Definition of the internal coordinate frame for the reactions: $CH_4 + XH_n \rightarrow CH_3 + HXH_n$ where XH_n stands for H, CH_3, NH_2, OH or F

Table 1. Geometrical parameters of the reactants, transition structures and products (Å and degrees)

Reactants and products:

	H_2	CH_3	CH_4	NH_2	NH_3	OH	H_2O	HF
Distance X—H	0.730	1.072	1.082	1.015	0.991	0.967	0.948	0.921
Angles H—X—H	—	120.0	109.5	108.6	116.1	—	111.5	—
Obtained Symm.	$D_{\infty}h$	D_3h	Td	C_2v	C_3v	$C_{\infty}v$	C_2v	$C_{\infty}v$

Experimental geometries

	H_2	CH_3	CH_4	NH_2	NH_3	OH	H_2O	HF
Distances X—H	0.742	1.079	1.085	1.024	1.012	0.971	0.957	0.917
Angles H—X—H	—	120.0	109.5	103.4	106.7	—	104.5	—

Transition structures:

With	H	CH_3	NH_2	OH	F
d_1	1.077	1.079	1.078	1.078	1.077
d_2	1.077	1.079	1.079	1.077	1.077
d_3	1.077	1.079	1.079	1.077	1.077
d_1	—	1.079	1.008	0.962	—
d_2	—	1.079	1.008	—	—
d_3	—	1.079	—	—	—
r_1	1.363	1.357	1.341	1.334	1.282
r_2	0.934	1.357	1.261	1.192	1.179
α_1	104.3	105.1	108.3	106.5	104.1
α_2	104.3	105.1	103.4	102.7	104.1
α_3	104.3	105.1	103.4	102.7	104.1
α'_1	—	105.1	104.8	104.6	—
α'_2	—	105.1	104.8	—	—
α'_3	—	105.1	—	—	—
β_1	114.1	113.5	113.6	114.3	114.3
β_2	114.1	113.5	113.6	114.3	114.3
β'_1	—	113.5	110.4	—	—
β'_2	—	113.5	—	—	—
δ	180.0	180.0	187.7	186.5	180.0
ϕ	180.0	180.0	180.0	180.0	180.0
Ω	—	180.0	58.1	180.0	—
found symmetry	C_3v	D_3d	Cs	Cs	C_3v

Related geometrical parameters:

C—X	2.297	2.714	2.596	2.521	2.461
γ	75.74	74.92	75.05	75.94	75.97

constrained. Nevertheless, except for NH_3 the standard deviation between experimental and theoretical geometries remains lower than 0.04 Å [27]. Let us now consider the transition structures. It appears that three of them (with H, CH_3 and F radicals) have a linear C···H···X structure. The two remaining (with NH_2 and OH radicals) are slightly bent (6.5 and 7.7 degrees respectively). We also

Table 2. Relative bond ratio for migrating hydrogen

	$r_{rel.1}$	$r_{rel.2}$	$r_{rel.1}/r_{rel.2}$
H	1.26	1.28	0.98
CH_3	1.25	1.25	1.00
NH_2	1.24	1.27	0.98
OH	1.23	1.26	0.98
F	1.18	1.28	0.92

see that the geometrical parameter r_1 do not vary largely. On the other hand r_2 depends on the nature of the attacking radicals. However, if we define the corresponding relative bond ratios $r_{rel.1}$ and $r_{rel.2}$ as follows:

$$r_{rel.1} = \frac{r_1}{d_{CH}(CH_4)} \quad \text{and} \quad r_{rel.2} = \frac{r_2}{d_{XH}(XH_{n+1})} \tag{3}$$

we obtain the results reported in Table 2. Those ratios are approximately constant. The mean value of $r_{rel.}$ for all the reactions equals 1.25 with a standard deviation of 0.028.

So for doublet transition structures the intersystem bond lengths are 25% larger than the corresponding lengths in equilibrium geometries. The same relative bond ratios lead for closed shell reactions to a bond length increase of 50% [28]. Finally we observe that the umbrella angle (γ) for the CH_3 fragment always remains close to 75.5°.

The other structural parameters do not vary widely between reactant and product structures. So, from a geometrical point of view it appears that the structural changes remain in agreement with the least change principle.

2. Vibrational analysis and thermodynamical properties

Making use of the local analytical surfaces around any stationary point, we can perform the vibrational analysis. In the quadratic approximation, the classical analysis leads to the same results as quantum mechanical calculations. So, using Wilson's method [29] we write:

$$L^{-1}GH_0L = \Lambda \tag{4}$$

$$\nu = \frac{1}{2\pi}(\Lambda)^{1/2}$$

with $S = LQ$, if L matrix diagonalizes the GH_0 product; G is the Wilson's matrix; ν are the vibrational frequencies; Q are the normal coordinates.

As already mentioned [30], the vibrational frequencies computed at SCF level using 6-31G basis set are overestimated by 10% compared to the experimental results. In Fig. 2, we show the correlation between experimental and theoretical values.

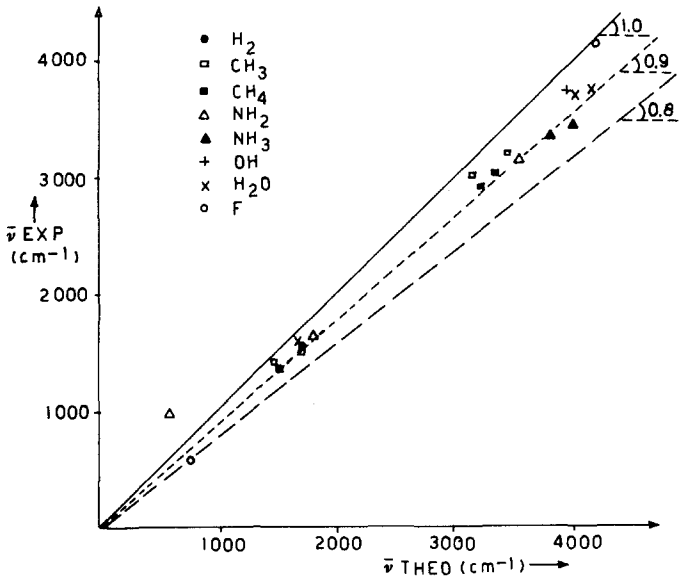

Fig. 2. Correlation between experimental [31] and theoretical frequencies of vibration for some small molecules

We obtain a regression line corresponding to the relation:

$$\nu_{exp} = 0.90887\tilde{\nu}_{th} + 37.36\ \text{cm}^{-1} \tag{5}$$

with a correlation coefficient of 0.991. This strong correlation between both sets of data is supposed to exist not only for equilibrium structures but also for the transition points where no experimental values are available. In Fig. 3, we give the results obtained for the transition structures. One observes the existence of imaginary frequencies (one per supermolecule). They correspond to the negative eigenvalues associated with the reaction coordinates through the transition saddle point. Among the real frequencies, some are of very low values (less than 100 cm^{-1}). They correspond, actually, to internal rotation instead of usual vibration motions. Below 600 cm^{-1}, we find some vibration modes which become translation and rotation degrees of freedom in the dissociated structures (the reactants and the products).

If now we consider the normal coordinates Q^* which correspond to the negative curvature of the surface at the transition point (see Table 3), we find that they are dominated by the combination $r_1 - r_2$.

The contribution of α and β type valence angles to Q^* is of minor importance. The associated angular motion corresponds in good approximation to the combination $\gamma - \gamma'$ of the umbrella deformations.

From Table 3, we can also calculate the angle between the r_1 direction and the projection of Q^* in the $r_1 r_2$ plane. We obtain 55°, 45°, 41°, 38° and 37° for the reactions with H, CH_3, NH_2, OH and F respectively. This shows that for H atom,

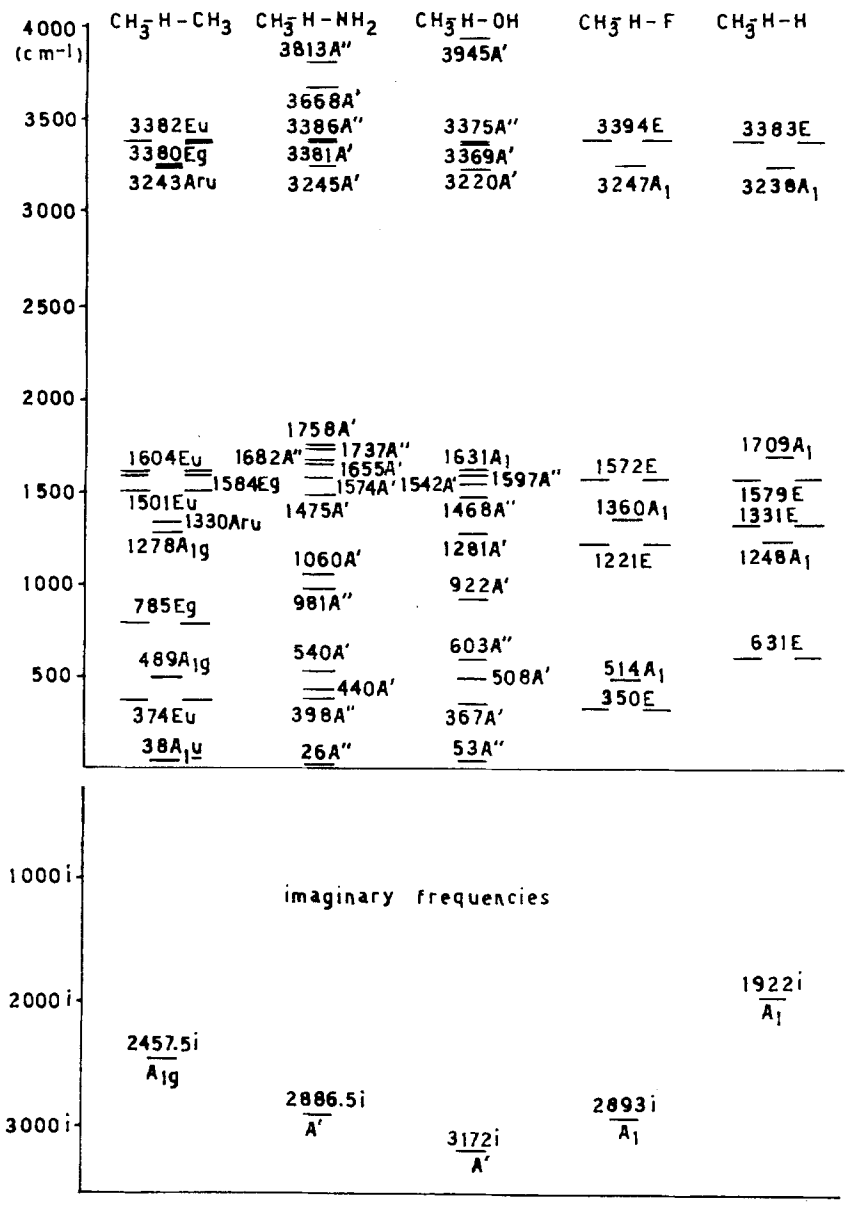

Fig. 3. Normal vibration frequencies (cm^{-1}) for the different transition structures

the transition point appears early on the reaction path (close to the reactants structure). On the other hand with $F^{\bullet}$ radical the transition point appears lately, i.e. the r_2 lowering is larger than the r_1 increase.

Let us now consider some thermodynamical properties directly related to the previous results. Application of statistical thermodynamics at the harmonic level

Table 3. Normal coordinate Q^* corresponding to the negative curvature of the surface at the transition point

$X-H_n$	$Q^* = L^{-1}(*)S$
H	$0.80r_1 - 0.56r_2 - 0.12(\alpha_1 + \alpha_2 + \alpha_3) + 0.06(\beta_1 + \beta_2)$
CH_3	$0.69(r_1 - r_2) - 0.09(\alpha_1 + \alpha_2 + \alpha_3 - \alpha'_1 - \alpha'_2 - \alpha'_3) + 0.04(\beta_1 + \beta_2 - \beta'_1 - \beta'_2)$
NH_2	$0.64r_1 - 0.73r_2 - 0.10(\alpha_1 + \alpha_2 + \alpha_3 - \alpha'_1 - \alpha'_2) + 0.03(\beta_1 + \beta_2) + 0.04\beta'$
OH	$0.61r_1 - 0.77r_2 + 0.09(\alpha_1 + \alpha_2 + \alpha_3 - \alpha'_1)$
F	$0.59r_1 - 0.79r_2 - 0.10(\alpha_1 + \alpha_2 + \alpha_3) + 0.03(\beta_1 + \beta_2)$

Table 4. Theoretical (and experimental [31]) thermodynamical properties at 298.15 K[a]

	Thermal corrections $H^0(T) - H^0(0)$ kcal mol^{-1}	Heat capacity C_p^0 cal mol^{-1} K^{-1}	Entropy S^0 cal mol^{-1} K^{-1}
H_2	8.72	6.96 (6.89)	31.05 (31.21)
CH_4	32.94	8.22 (8.52)	44.36 (44.48)
NH_3	25.31	9.04 (8.52)	46.18 (46.03)
OH_2	16.39	7.99 (8.03)	44.93 (45.11)
FH	8.01	6.96 (6.96)	41.46 (41.51)
H	1.48	4.97 (4.97)	27.39 (27.39)
CH_3	21.70	8.81 (9.25)	46.06 (46.38)
NH_2	15.07	7.99 (8.02)	46.36 (46.50)
OH	7.73	6.96 (7.17)	42.53 (43.88)
F	1.48	4.97 (5.44)	36.15 (37.92)
CH_3-H-H	31.23	10.48	51.58
CH_3-H-CH_3	53.13	15.27	64.53
CH_3-H-NH_2	47.23	13.98	63.76
CH_3-H-OH	37.24	13.61	64.23
CH_3-H-F	29.00	12.93	59.57

[a] For transition structures, the imaginary frequencies have been discarded.

(for vibration motions) is quite simple [30]. On Table 4, we report the computed thermal corrections, heat capacities and entropies at 298.15 K. When comparison with experimental data is feasible, we obtain satisfactory agreement. Linear correlation (with slope close to one) such as that given by relation (5) exists also for the present thermodynamical properties.

3. The energetic point of view

One knows that SCF energies are not sufficiently accurate to give valuable transition barriers and *a fortiori* reaction energies [32]. Using SCF stationary structures, we have further performed some CI calculations. The following strategy has been employed:

(1) UHF molecular orbitals have been transformed [33] to an RHF molecular basis set (C^{RHF}) by diagonalizing the projector (R) to the occupied space:

$$R = V\,\mathrm{SDS}\,V' \tag{6}$$

where D is the total UHF density matrix: $D = D^{\alpha} + D^{\beta}$; V is the Löwdin's orthogonalization matrix [34]; S is the overlap matrix in terms of atomic orbitals.

If

$$U'RU = \eta(\text{diagonal})$$

then

$$C^{\text{RHF}} = UV. \tag{7}$$

The UHF occupation number (η) obtained in this way are not exactly integers but are close to zero, one or two. It follows that RHF energies are not quite different to the UHF ones (E(RHF) slightly higher then E(UHF)).

(2) The CI is then performed using the Huron–Malrieu's iterative scheme [35]. At any step the multiconfigurational zeroth order wave-function forms a strong interacting subspace of the configuration space. In the complementary space, the configuration interaction is performed on a perturbational way. Then configurations which have a first order perturbational CI coefficient greater than a given threshold (T) are added to the zeroth order wave-function for the next iteration.

(3) Iteration process was repeated decreasing the threshold T to 0.005. At this level the wave-function contains between 200 and 800 configurations depending on the system we study. Natural orbitals [36–37] are then computed in order to improve our reference determinant (C^{NO} replaces C^{RHF}).

(4) In the NO basis set, 5 to 15 references configurations are selected by scheme 2. The configurations lying in the complementary space are ordered according to their perturbation CI coefficients. Diagonalization is then performed at different selection threshold; it enabled us to use a modified Buenker–Peyerimhof [38] extrapolation at zero threshold:

$$E(T) = E_0 + \lambda T^{\sigma}. \tag{8}$$

The curve $E(T)$ has a quasi linear shape. The σ parameter enables us to adjust the slight curvature of the function $E(T)$. The fitting is carried out by the simplex method [39].

This strategy enabled us to obtain energies as good as possible without too expansive computations. Results obtained are reported in Table 5 for absolute values and in Table 6 for relative values.

We note that the reaction energies become better at CI level but remain different from the experimental values by 3 to 20 kcal mol^{-1}. For transition barriers, the comparison is difficult. Assuming no tunneling corrections, we can obtain from last column of Table 5 and from thermal corrections given in Table 4 the estimated transition barriers of Table 6. We see that theoretical values are larger than the previous estimations by 2 to 6 kcal mol^{-1}. As tunnel effect must decrease those barriers by a few kcal mol^{-1}, it appears that theoretical $\Delta E^{(\neq)}$ are in some agreement with experimental data. At least the reactions are well ordered.

Table 5. Total energies (in Hartrees) at different level of approximation

	E(UHF)	E(HF limit) [40]	E(CI)[a]	E(extr)	E(exp) [41]
H_2	−1.12683	−1.1336	−1.15152 (10)	−1.15152	−1.1744
CH_4	−40.18055	−40.219	−40.29069 (997)	−40.29260	−40.526
NH_3	−56.16552	−56.226	−56.28537 (913)	−56.28750	−56.588
OH_2	−75.98536	−76.068	−76.11729 (819)	−76.11736	−76.483
FH	−99.98343	−100.072	−100.11222 (988)	−100.11222	−100.533
H	−0.49823	−0.500	—	—	−0.500
CH_3	−39.54666	−39.584	−39.63790 (915)	−39.63947	−39.846
NH_2	−55.55331	−55.591	−55.61463 (152)	−55.63231	−55.911
OH	−75.36318	−75.426	−75.46154 (872)	−75.46154	−75.783
F	−99.36086	−99.415	−99.44823 (865)	−99.44823	−99.809
CH_3—H—H	−40.63998	—	−40.75229 (968)	−40.76502	—
CH_3—H—CH_3	−79.67990	—	−79.80034 (962)	−79.90067	—
CH_3—H—NH_2	−95.66352	—	−95.82929 (960)	−95.89932	—
CH_3—H—OH	−115.49267	—	−115.67862 (919)	−115.73600	—
CH_3—H—F	−139.49924	—	−139.69512 (966)	−139.72906	

[a] Energy (determinant number).

Table 6. Relative energies (kcal mol^{-1}) at different levels

Reaction energy: $\Delta E(R)$				
	UHF	HF limit	CI+Ext	Exp. f.n.
CH_3—H—H	3.32	0.88	−0.10	3.51
CH_3—H—CH_3	0.00	0.00	0.00	0.00
CH_3—H—NH_2	13.61	0.00	−1.29	1.88
CH_3—H—OH	7.30	−4.40	−1.68	−12.54
CH_3—H—F	7.10	−13.80	−6.81	−27.72

Transition energy: $\Delta E^{(\neq)}$				
	UHF	CI+Ext.	Estim. f.n.	E_a(exp) 298.15 K[a]
CH_3—H—H	24.74	16.19	9.9	11.9 (9.6–12.2) [42]
CH_3—H—CH_3	29.90	19.69	14.3	14.0 (14.1–14.7) [43]
CH_3-H-NH_2	36.86	16.05	9.9	10.3 (10.3–11.8) [44]
CH_3—H—OH	31.35	11.38	6.0	3.77 (3.4–5.0) [45]
CH_3—H—F	26.73	7.38	5.4	1.15 (1.1–1.9) [46]

[a] Recommended activation energy at 298.15 K.

4. Rate constant calculation

As we dispose of the local analytical potential surface in reactant and transition regions, we can compute the reaction rate constant in the so-called transition state approximation. If the second order rate constant is expressed in units of volume per mole and unit of time we can use the following equation [47–48]:

$$k(T) = \frac{\chi T^2}{h} \frac{R'}{P} \exp\left(\frac{\Delta S^{\neq}}{R}\right) \exp\left(-\frac{\Delta H^{\neq}}{RT}\right) \tag{9}$$

where χ is the Boltzman's constant; R is the perfect gas constant; R' has same meaning as R but may be expressed in other units; P and T are respectively the pressure and temperature; $\Delta S^{\neq}$ and $\Delta H^{\neq}$ are the molar entropy and enthalpy change between reactants and transition point.

According to the previous relation the activation energy (also called Brönsted slope) is defined by:

$$E_a = RT^2\left(\frac{d\ln k}{dT}\right)_P = \Delta H_0^{\neq} + 2RT = \Delta E_0^{\neq} + RT. \tag{10}$$

The usual Arrhenius expression becomes:

$$k(T) = A\exp\left(-\frac{E_a}{RT}\right) \tag{11}$$

with

$$A = \frac{\chi T^2}{h}\frac{e^2 R'}{P}\exp\left(\Delta S^{\neq}/R\right). \tag{12}$$

Tunnel correction can be included by introducing in (9) a tunneling factor x. At first approximation, Wigner has evaluated this factor as [49]:

$$x(W) = 1 + \frac{1}{24}\left(\frac{h\nu^{\neq}}{kT}\right)^2 \tag{13}$$

where $\nu^{\neq}$ stands for the imaginary frequency.

Christov obtains from a more elaborated treatment an alternate expression for x [50]:

$$x(C) = \frac{2}{2-d}\left\{1 - \frac{d}{2}\exp\left\{b(d-2)\right\}\right\} \tag{14}$$

where $d = T_c/T$; $b = \{\Delta E^{\neq} - \Delta E(R)\}/T_c$ for $\Delta E^{\neq} \geq \Delta E(R)$; $T_c = h\nu^{\neq}/\pi$ (critical temperature).

The Christov's correction is only valuable if the temperature is greater than half of T_c. The final rate constant and activation parameters become:

$$k^*(T) = xk(T) = A^*\exp\left(-\frac{E_a^*}{RT}\right) \tag{15}$$

with, for Wigner:

$$E_a^* = E_a - 2RT(\pi d)^2/\{24 + (\pi d)^2\}$$

or for Christov:

$$E_a^* = E_a - RT_c\left[\frac{1}{2-d} - \frac{(1+d)\exp\left\{b(d-2)\right\}}{2 - d\exp\left\{b(d-2)\right\}}\right]$$

Table 7. Magnitude of the tunneling correction on the activation energy (E_a) and on the preexponential factor (A) assuming a critical temperature (T_c) of 880 K

$T(K)$	Wigner's correction			Christov's correction		
	$\log(x)$	$E_a^*-E_a$	$\ln(A^*/A)$	$\log(x)$	$E_a^*-E_a$	$\ln(A^*/A)$
440 ($-T_c/2$)	0.423	−1.09	−0.12	1.292	−8.52	−2.94
880 ($=T_c$)	0.150	−1.02	−0.10	0.301	−1.75	−0.13
1760 ($=2T_c$)	0.043	−0.65	−0.04	0.125	−1.17	−0.02
3520 ($=4T_c$)	0.011	−0.35	−0.01	0.058	−1.00	−0.00

Table 8. Some parameters for the studied abstraction reactions, at 298.15 K[a]

CH_4+R	$R=H$	$R=CH_3$	$R=NH_2$	$R=OH$	$R=F$
$\Delta E_0^{\neq}(T)$ kcal mol^{-1}	13.59	18.76	15.87	8.54	2.55
E_a(tst) kcal mol^{-1}	14.18	19.35	16.46	9.13	3.14
T_c K	880.2	1125.5	1322.0	1452.7	1324.9
E_a^*(Wig) kcal mol^{-1}	13.17	18.30	15.39	8.18	2.21
E_a(exp) kcal mol^{-1}	11.90	14.00	10.30	3.77	1.15
$\Delta S_0^{\neq}$ cal mol^{-1} K^{-1}	−20.17	−25.89	−26.96	−22.67	−20.94
$\Delta Cp_0^{\neq}$ cal mol^{-1} K^{-1}	−2.71	−1.76	−2.23	−1.57	−0.25

[a] Christov's E_a^* is not given because 298.15 K is less than $T_c/2$.

and, for both:

$$\ln A^* = \ln(A) + \left\{ \ln(x) + \frac{E_a^* - E_a}{RT} \right\}.$$

As shown in Table 7, tunneling corrections are of some importance in the range $T_c/2$ to $2T_c$.

In Table 8, we report the values of some activation parameters. It is seen that critical temperatures are relatively large (in the range [880, 1450] cm^{-1}). So the room temperature is never a temperature for which relation (9) gives satisfactory results. At this temperature the Wigner's correction is certainly too small and the Christov's equations are invalid.

Comparison has to be performed at higher temperature. In Table 9, we give the rate constants for different values of T. The standard deviation between log k^* (Christov) and log k (exp) is less than 0.3 (as long as $T \geq T_c/2$).

In the extreme cases on the T_c scale, we report more details for the $k(T)$ function in Figs. 4 and 5. In those cases as in the others, we obtained a non-Arrhenius behavior. This coincides with experimental results reviewed by Shaw [63] and Zellner [65]. Present results suggest that the non-Arrhenius behavior exists without tunneling corrections. Nevertheless, the latter increases the curvature of the $k(T)$ function. If we obtain non-Arrhenius behavior in all cases, this effect is rather small particularly in the case of reaction with CH_3 radical. We may

Table 9. Rate constants with and without tunneling corrections at different temperatures

Reactions[a]	$T(K)$	$\log(k)$ (9)	$\log(k^*)$ Wigner	$\log(k^*)$ Christov	$\log(k)$ exp.	Ref.
CH_4+H	1852	12.66	12.70	12.78	13.04	[51]
	1695	12.45	12.50	12.58	12.85	[52]
	1610	12.31	12.36	12.45	12.51	[53]
	1000	10.92	10.97	11.10	11.10	[54]
	730	9.60	9.80	10.00	10.36	[55]
	370	4.78	5.30	7.09	7.37	[56]
CH_4+CH_3	800	7.40	7.66	7.93	7.75	[57]
	593	5.48	5.87	6.56	6.53	[58]
	500	4.00	5.49	5.87	5.49	[59]
CH_4+NH_2	500	5.33	5.92	7.65	7.20	[44]
CH_4+OH	2000	13.13	13.22	13.33	13.00	[60]
	1300	12.22	12.40	12.57	12.70	[61]
	1200	12.03	12.23	12.42	12.00	[62]
	930	11.68	11.98	12.27	12.61	[63]
	298		7.47	—	9.71	[64]
CH_4+F	298		11.90	—	13.66	[46]

[a] Rate constants are in $cm^3\ mol^{-1}\ sec^{-1}$ at 1 atm pressure.

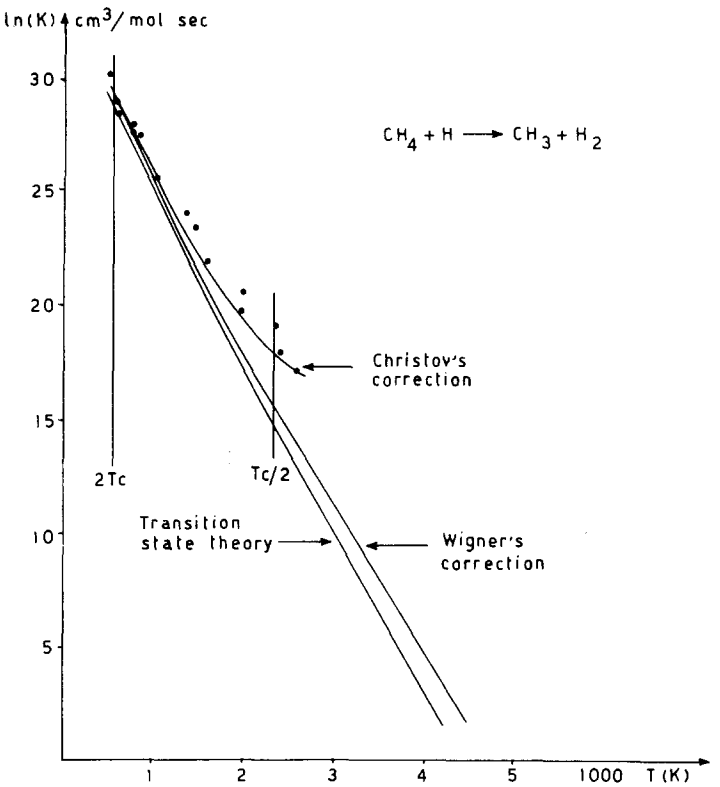

Fig. 4. Rate constant for the abstraction reaction $CH_4+H \rightarrow CH_3+H_2$ (heavy curves are theoretical and points, experimental)

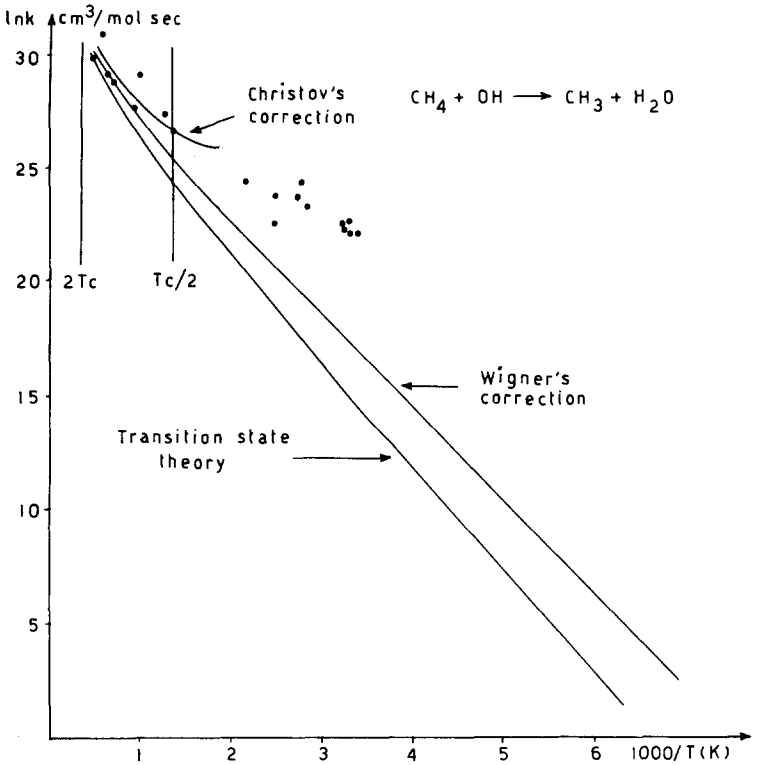

Fig. 5. Rate constant for the abstraction reaction $CH_4 + OH \rightarrow CH_3 + H_2O$ (heavy curves are theoretical and points, experimental)

propose the following order in decreasing curvature magnitude:

$$F > OH > H > NH_2 > CH_3.$$

This order also coincides with decreasing reaction rate. Figs. 4 and 5, as well as Table 9, show that above $T_c/2$ theoretical and experimental values are rather close. This agreement may be due to some cancellation of errors in the theoretical results. Nevertheless, it seems that one can relatively easily obtain acceptable results.

5. Conclusions

In the study of hydrogen abstraction reactions, the inclusion of correlation by means of a CIPSI-INO iterative scheme, with non-linear extrapolation of the energies gives more or less reliable results as compared to experience. Also, the optimization procedure based on the local fitting of an all-parameter quadratic hypersurface seems to work well even for a large number of internal degrees of freedom.

From a geometrical point of view it is found that the transition states for the five reactions studies are very similar. The C—H methyl distances and umbrella angles are almost the same.

The more interesting geometrical changes at the transition states are those of r_1 and r_2. We see that the values of r_1 increase steadily in the sequence $F < CH < NH_2 < CH_3 < H$. This is exactly the experimental sequence of decreasing exothermicity, so Hammond's postulate seems to bear a relation to the deformation of the bond which is breaking in the reaction. We also note the similar behavior of relative distance $r_{rel.1}$ with respect to exothermicity.

On the other hand, the distance H—X corresponding to the bond which is forming, does not seem to bear a clear relationship to exothermicity. The ratio $r_{rel.1}/r_{rel.2}$ gives for the exactly thermoneutral reaction a value of 1, and for the strongly exothermic reaction with F a value of 0.92, corresponding clearly to an increase of reactant-likeness.

Perhaps more clearly, the relative deformation measured by the angle of inclination of the transition vector in the $r_1 - r_2$ plane follows the same ordering of the experimental heats of reaction. The reactant likeness of the transition structure leads to activation barriers which are not too bad. Then the vibrational and thermodynamical analysis enable us to apply the transition state theory. It appears that at very high temperature it gives quite acceptable results. At lower temperature, tunneling corrections are required. Christov's relation seems to provide results close to experiments as long as the temperature is above $T_c/2$. In all cases we find a non-Arrhenius behavior even before tunneling corrections.

In a further work, we will consider a larger set of abstraction reactions in order to explore more deeply the relations between activation parameters and some reactants properties such as, for example, bond dissociation energies, ionization potential and electron affinity, ...

Acknowledgement. One of us (JLV) wishes to thank the "Secrétariat du Tiers Monde de l'Université Catholique de Louvain" for financial support which allowed him to pursue this research.

References

1. Leroy, G., Wilante, C., Peeters, D., Khalil, M.: Ann. Soc. Scient. Bruxelles **95**, 157 (1981)
2. Shaw, R.: J. Phys. Chem. Ref. Data **7**, 1179 (1978)
3. Davis, D. D., Fischer, S., Schiff, R.: J. Chem. Phys. **61**, 2213 (1974)
4. Wilson, W. M. E.: J. Phys. Chem. Ref. Data **1**, 559 (1972)
5. Trotmann-Dickenson, A. F.: Advances in Free-Radical Chemistry, Vol. 1, Logos Press (1965)
6. Zellner, R.: J. Phys. Chem. **83**, 18 (1979)
7. Gray, P., Herod, A. A., Jones, A.: Chem. Rev. **71**, 247 (1971)
8. Kerr, J. A., Parsonage, M. J.: Evaluated Kinetic Data of Gas Phase Hydrogen Transfer Reactions of Methyl Radicals. Butterworths 1976
9. Fukui, K., Kato, S., Fujimoto, H.: J. Amer. Chem. Soc. **97**, 1 (1975)
10. Ishida, K., Morokuma, K., Komornicki, A.: J. Chem. Phys. **66**, 2153 (1977)
11. Niblaeus, K., Roos, B. O., Siegbahn, P. E. M.: Chem. Phys. **26**, 59 (1977)

12. Hase, W. L., Mrowka, G., Brodzynski, R. J.: J. Chem. Phys. **69**, 3548 (1978)
13. Dewar, M. J. S., Olivella, S.: J. Amer. Chem. Soc. **100**, 5290 (1978)
14. Nagase, S., Morokuma, K.: J. Amer. Chem. Soc. **100**, 1666 (1978)
15. Rayez-Meaume, M. T., Dannenberg, J. J., Whitten, J. L.: J. Amer. Chem. Soc. **100**, 747 (1978)
16. Shinohara, H., Imamura, A., Masuda, T., Kondo, M.: Bull. Chem. Soc. Japan **51**, 1917 (1978)
17. Shinohara, H., Imamura, A., Masuda, T., Kondo, M.: Bull. Chem. Soc. Japan **52**, 974 (1979)
18. Carsky, P.: Collect. Czechosl. Chem. Comm. **44**, 3452 (1979)
19. Carsky, P., Zahradnik, R.: J. Mol. Structure **54**, 247 (1979)
20. Hehre, W. J., Ditchfield, R., Pople, J. A.: J. Chem. Phys. **56**, 2257 (1972)
21. Pople, J. A., Nesbet, K.: J. Chem. Phys. **22**, 571 (1954)
22. Hehre, W. J., Lathan, W. A., Ditchfield, R., Newton, M. D., Pople, J. A.: QCPE 236
23. Schlegel, H. B.: FORCE program, according to the method of Pulay; Pulay, P.: Mol. Phys. **17**, 197 (1969); Schlegel, H. B.: in Computational theoretical organic chemistry, Csizmadia, I. G., Daudel, R. Eds. Reidel 1981
24. Fedorov, V.: Theory of optimal experiments. New York: Academic Press, 1972
25. Sana, M.: Intern. J. Quantum Chem. **19**, 139 (1981)
26. Sana, M.: Theoret. Chim. Acta (Berl.) **60**, 543 (1982)
27. Standard deviation between two geometries can be obtained as follows: place the origin of the cartesian coordinates at the center of mass of both molecules; orient them properly according to the principal components of their inertial tensor; then if $\vec{r}_1(i)$ and $\vec{r}_2(i)$ are the position vector of the atom "i" in both structures:

$$s=\left\{\frac{1}{k}\sum_{i=1}^{N}[\vec{r}_1(i)-\vec{r}_2(i)]^2\right\}^{1/2}$$

for $k=3N-6$ or $3N-5$
28. Sana, M.: unpublished results (1983)
29. Wilson, E. B., Decius, G. C., Cross, P. C.: Molecular vibrations. New York: McGraw Hill, 1955
30. Sana, M.: in Computing Theoretical Organic Chemistry, Csizmadia, I. G., Daudel, R., Eds. p. 183. Dordrecht: Reidel, 1981
31. Stull, D. R., Prophet, N.: Janaf Thermochemical Tables. Washington D.C.: National Bureau of Standards, 1971
32. Leroy, G., Sana, M.: Ann. Soc. Scient. Bruxelles **92**, 79 (1978)
33. Daudel, R., Leroy, G., Peeters, D., Sana, M.: Quantum chemistry. Chichester: Willey, in press
34. Löwdin, P. O.: J. Chem. Phys. **18**, 365 (1950).
35. Huron, B., Malrieu, J. P., Rancurel, P.: J. Chem. Phys. **58**, 5745 (1973), Program CIPSI
36. Bender, C. F., Davidson, E. R.: J. Chem. Phys. **70**, 2675 (1968)
37. Sana, M.: QCPE Bull., RHO1 (1983)
38. Buenker, R. J., Peyerimhof, S. D.: Theoret. Chim. Acta (Berl.) **35**, 33 (1974); Theoret. Chim. Acta (Berl.) **39**, 217 (1975); Buenker, R. J., Peyerimhof, S. D., Butscher, W.: Mol. Phys. **35**, 771 (1978)
39. Nelder, J. A., Mead, R.: Computer J. **7**, 308 (1965)
40. Pople, J. A.: in Applications of Electronic Structure Theory, ed. H. F. Shaeffer III. New York: Plenum Press 1977
41. Pople, J. A., Binkley, J. S.: Mol. Phys. **29**, 599 (1975)
42. Baldwin, R. R., Walker, R. W.: J. Chem. Soc. Perkin II, 361 (1973)
43. Kerr, J. A., Parsonage, M. J.: Evaluated Kinetic Data of Gas Phase Hydrogen Transfer Reactions of Methyl Radicals. Butterworths 1976
44. Demissy, M., Lesclaux, R.: J. Amer. Chem. Soc. **102**, 2898 (1980)
45. Greiner, N. R.: J. Chem. Phys. **53**, 1070 (1970)
46. Foon, R., Kaufmann, M.: Prog. React. Kinetics **8**, 81 (1975)
47. Daudel, R.: Quantum Theory of Chemical Reactivity. Boston: Reidel, 1973
48. Benson, S. W.: Thermochemical Kinetics. New York: Wiley 1976; Golden, D. W.: J. Chem. Phys. **48**, 235 (1971)
49. Wigner, E. P.: Phys. Chem. **B19**, 203 (1933)

50. Christov, S. G.: Collision Theory and Statistical Theory of Chemical Reactions, Lecture Notes in Chemistry **18**. New York: Springer Verlag, 1980
51. Roth, P., Just, Th.: Ber. Bunsen Ges. **79**, 682 (1975)
52. Biordi, J. C., Lazzara, C. P., Papp, J. F.: Comb. and Flame **26**, 57 (1976)
53. Benson, S. W., Golden, D. M., Laurence, R. W., Shaw, R., Woolfolk, R. W.: Intern. J. Chem. Kin. Symp. **no. 1**, 399 (1975)
54. Bush, S. F., Dyer, P.: Proc. Roy. Soc. (London) **A351**, 33 (1976)
55. Kurylo, M. J., Hollinden, G. A., Timmons, R. B.: J. Chem. Phys. **52**, 1773 (1970)
56. Berlie, M. R., LeRoy, D. J.: Can. J. Chem. **32**, 650 (1954)
57. Trotmann-Dickenson, A. F., Steacie, E. W. R.: J. Phys. Colloid Chem. **55**, 908 (1951)
58. Wijnen, M. H. J.: J. Chem. Phys. **23**, 1357 (1955)
59. Dainton, F. S., Ivin, K. J., Wilkinson, F.: Trans. Faraday Soc. **55**, 929 (1959); Demissy, M., Lesclaux, R.: J. Amer. Chem. Soc. **102**, 2898 (1980)
60. Wilson, W. E., O'Donovan, J. T., Fristrom, R. M.: 12th Combustion see Shaw, R. J.: Phys. Chem. Ref. Data **7**, 1179 (1978)
61. Bradley, J. N., Capey, W. D., Fair, R. W., Pritchard, D. K.: Intern. J. Chem. Kin. **8**, 549 (1976)
62. Pratt, N. H.: 11th Combustion Symposium, see Shaw, R.: J. Phys. Chem. Ref. Data **7**, 1179 (1978)
63. Shaw, R.: J. Phys. Chem. Ref. Data **7**, 1179 (1978)
64. Gordon, S., Mulac, W. A.: Intern. J. Chem. Kin. Symp. **1**, 289 (1975)
65. Zellner, R., Steinert, W.: Intern. J. Chem. Kin. **8**, 397 (1976)

Received October 11, 1983